Journal of Materials Chemistry C

Mechanochromic Luminescence of Halide-Substituted Difluoroboron β-Diketonate Dyes

Journal:	*Journal of Materials Chemistry C*
Manuscript ID:	TC-ART-10-2014-002268.R1
Article Type:	Paper
Date Submitted by the Author:	03-Nov-2014
Complete List of Authors:	Morris, William; University of Virginia, Department of Chemistry Liu, Tiandong; University of Virginia, Department of Chemistry Fraser, Cassandra; University of Virginia, Department of Chemistry

Mechanochromic Luminescence of Halide-Substituted Difluoroboron β-Diketonate Dyes

William A. Morris, Tiandong Liu, and Cassandra L. Fraser

Department of Chemistry, University of Virginia, McCormick Road, Charlottesville, VA 22904

To whom the correspondence should be addressed. E-mail: fraser@virginia.edu

ABSTRACT

Many difluoroboron β-diketonate (BF_2bdk) compounds display mechanochromic luminescence (ML) and substituents can influence their optical properties. For example, the difluoroboron iododibenzoylmethane derivative, BF_2dbm(I)$OC_{12}H_{25}$, exhibits mechanochromic luminescence quenching (MLQ). When annealed films of this dye are smeared under air, the perturbed region becomes dim under UV light. In this study, effects of differing halide substituents on ML were investigated. A series of dyes of the form BF_2dbm(X)$OC_{12}H_{25}$, where X = H, F, Cl, Br, and I, were synthesized. The luminescence properties of these dyes were studied in CH_2Cl_2 solution, as films on weighing paper, spin-cast films on glass substrates, and as bulk powders. All of the dyes exhibit ML and MLQ. Solid-state emissions from these dyes are also sensitive to annealing temperature. The F, Cl, and Br dyes required higher annealing temperatures than the H and I analogues to achieve ordered emissive states. Spin-cast films of the dyes on glass were studied using atomic force microscopy (AFM) and X-ray diffraction (XRD), revealing a change from an amorphous material in the as-spun state to an ordered, crystalline material after annealing, with the F and Cl dyes showing a propensity to form large lamellar crystallites. Powders were also investigated using XRD and showed changes in diffraction patterns corresponding to thermal annealing and grinding. Finally, halogen substituents greatly diminished the ability of the dye films to recover their ordered emissive states after smearing under ambient conditions. These dyes could be useful for applications in which a more permanent inscription is desirable.

INTRODUCTION

Materials that are responsive to external force stimuli are of interest to the scientific and technological communities due to their potential for use in sensors, memory storage, security inks, and other applications.[1-5] But the design of mechanofunctional materials with predictable and tunable properties remains a challenge and cutting edge area of materials science.[1,2] Mechanochromic luminescent (ML) materials[1-5] change luminescence color in response to mechanical perturbation. There are several classes of ML materials including liquid crystals,[6,7] polymers,[3,8,9] inorganic and organic molecular solids,[10,11] and even micelles.[12] Since emission in the solid state is required for ML, many materials also belong to a class of compounds that exhibit aggregation-induced emission (AIE) and aggregation-induced enhanced emission (AIEE).[1,13-15] This makes them potentially useful for many more applications including OLED development and even tracking of drug delivery.[16-18]

Previously, Kato *et al*. reported that pyrene-based liquid crystals display mechanochromism *via* a shear force-induced phase transition from a micellar cubic phase to a columnar phase.[6] Park *et al.* also made important advances in designing mechanical responsive materials.[19] Recently, they reported polymorphism as well as ML behavior in emissive dicyanodistyrylbenzene crystals.[20] Typically, proposed mechanisms for ML involve a change in intermolecular interactions that can be brought about by mechanical force.[2,6,20-22] More recently, Tian *et al*. have reported that tetrakis(4-dimethylamino)phenyl)ethylene (TDMAPE), which has a natural propeller structure, displays a red-shift in emission due to a change in intramolecular conformation when

powders of the material are ground.[23] The blue-shifted emission of the pristine powders can be fully recovered by fuming with solvent or partially recovered by annealing.[23]

Difluoroboron β-diketonate (BF_2bdk) dyes are another class of materials known for their impressive optical properties. These include two-photon absorption cross-sections,[24,25] high extinction coefficients,[25-27] efficient quantum yields,[25-27] tunable absorption in the near-UV range,[25,27] a range of emission colors in the solid state,[27,28] intramolecular charge transfer character,[26,29] oxygen-sensitive room temperature phosphorescence in rigid media such as polymers,[30,31] organic vapor sensitivity,[32,33] and ML.[28,34-36] Previously we reported that BF_2bdk dyes display reversible ML and that alkoxy chain substituents of varying length can have significant effects on ML properties.[35,36] Atomic Force Microscopy (AFM) data revealed a change from a more ordered state to an amorphous one upon perturbation of the dye materials.[35] We also reported that an iodine heavy atom substituent can facilitate mechanically induced luminescence quenching (MLQ).[37] Fluorescence intensity is diminished by enhanced crossover to the triplet state, which is sensitive to and thus, quenched by oxygen. Specifically, (BF_2dbm(I)$OC_{12}H_{25}$), a lipid derivative of difluoroboron iododibenzoylmethane, exhibited green fluorescence in the solid state under UV light after thermal annealing (TA).[37] Upon application of shear force (e.g. smearing), the emission from the dye became noticeably less intense at room temperature under air.[37] The dye also exhibited both fluorescence and phosphorescence (dual emission) at 77K in liquid N_2.[37] Smearing greatly altered the fluorescence to phosphorescence ratio (F/P) in favor of the more red-shifted phosphorescence, presumably by creating aggregates with S_1 excited states that are closer in energy to the aggregate T_1 state.[37]

Zhang *et al*. postulated that smearing of similar annealed BF_2bdk dyes leads to the formation of ground state and excimeric aggregate species.[21] Among these were proposed ground-state H-aggregates in which the BF_2bdk molecules adopt a face-to-face arrangement and exhibit blue-shifted absorption bands as well as red-shifted emission maxima. H-aggregates have a lower energy singlet excited state (S_1) than the more ordered polymorphs and could serve as acceptors for migrating excitons (an electron-hole pair).[21,38] Therefore, even if all molecules in the system do not adopt the lower energy conformation, the overall emission from the perturbed region of the material can be red-shifted. The iodide heavy atom also facilitates intersystem crossing between the S_1 and T_1 excited states of the fluorophore, leading to even further enhanced emission from the aggregate T_1 excited state (phosphorescence).[37,39]

However, many questions about these dyes remain unanswered, especially concerning MLQ and heavy atoms. To what extent does the heavy atom dictate whether or not a dye will show MLQ? How does the presence of a heavy atom affect the formation of the ordered emissive state as well as the amorphous state brought about by smearing? How do different halide substituents influence spontaneous recovery of the dyes at room temperature after smearing?

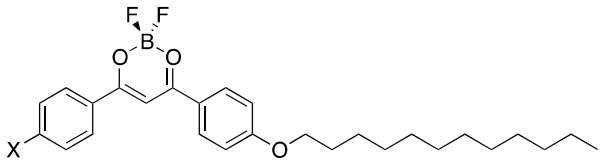

Fig. 1 Chemical structure of BF_2dbm(X)$OC_{12}H_{25}$ dyes (X = H, F, Cl, Br, or I).

To begin to address some of these questions, a series of dyes of the form $BF_2dbm(X)OC_{12}H_{25}$, where X = H, F, Cl, Br, or I (Fig. 1) were synthesized. By altering the halide substituent the effect of varying the weight of the substituent on ML and MLQ was explored. The dyes were studied in CH_2Cl_2 solution, as films on both weighing paper and glass substrates, and as bulk powders. The weighing paper substrate was utilized to study MLQ properties of the dyes at room and low temperature. Spin-cast films of the dyes on glass were used to monitor spontaneous recovery of the dyes at room temperature, for solid-state quantum yield measurement, atomic force microscopy (AFM) imaging, and X-ray diffraction (XRD) characterization. Dyes as bulk powders were studied by XRD to find structural differences between as-isolated (AI) powders, thermally annealed (TA) powders, and powders ground (GR) using a mortar and pestle.

EXPERIMENTAL

Materials

4-Dodecyloxyacetophenone was synthesized via a Williamson ether synthesis as previously reported.[36] Solvents CH_2Cl_2 and THF were either dried and purified by passage through alumina columns or dried over 3 Å molecular sieves according to a previously reported method.[40] All other chemicals were reagent grade from Sigma Aldrich and were used without further purification.

Methods

^{1}H NMR (300 MHz) spectra were recorded on a UnityInova 300/51 instrument in $CDCl_3$. ^{1}H NMR spectra were referenced to the signal for the chloroform residual proton at 7.26 ppm and coupling constants are given in Hertz. Mass spectra were recorded using an Applied Biosystems 4800 spectrometer with a MALDI TOF/TOF analyzer. Melting

points were recorded on a Mel-Temp II by Laboratory Devices, USA. UV/vis spectra were recorded on a Hewlett-Packard 8452A diode-array spectrophotometer. Steady-state fluorescence emission spectra were recorded on a Horiba Fluorolog-3 Model FL3-22 spectrofluorometer (double-grating excitation and double-grating emission monochromator). A 2 ms delay was used when recording the delayed emission spectra. Time-correlated single-photon counting (TCSPC) fluorescence lifetime measurements were performed with a NanoLED-370 (λ_{ex} = 369 nm) excitation source and a Datastation Hub as the SPC controller. Phosphorescence lifetimes were measured with a 1 ms multi-channel scalar (MCS) excited with a pulsed xenon lamp (λ_{ex} = 369 nm; duration < 1 ms). Lifetime data were analyzed with Datastation version 2.6 software from Horiba Jobin Yvon. Fluorescence quantum yields (φ_F) in CH_2Cl_2 solution were referenced *versus* quinine sulfate in 0.1 M H_2SO_4 as a standard according to a previously described method.[41] The following values were used: φ_F quinine sulfate = 0.54[42], n_D^{20} 0.1 M H_2SO_4 = 1.33, n_D^{20} CH_2Cl_2 = 1.424. Quantum yields for BF_2dbm(I)$OC_{12}H_{25}$ and BF_2dbm(H)$OC_{12}H_{25}$ were previously reported.[36,37] Optically dilute CH_2Cl_2 solutions of the dyes were prepared in 1 cm path length quartz cuvettes with absorbance <0.1 (a.u.). Solid-state quantum yields of spin-cast films were measured using a Quanta-φ F-3029 Integrating Sphere from Horiba Jobin Yvon. The Data was analyzed using FlourEssence software V 2.1 also from Horiba Jobin Yvon.

Films on weighing paper were created by smearing a small amount of dye onto 5 x 5 cm^2 pieces of weighing paper with nitrile examination gloves. After this, the samples were weighed to ensure a dye mass of ~1-3.5 mg spread out over the entire 5 x 5 cm^2 area. The films were annealed for 10 min in a Thermo Heratherm oven according to

the respective optimum annealing temperatures (determined experimentally) (H = 110 °C, F = 142 °C, Cl = 150 °C, Br = 140 °C, I = 110 °C).[28] A Laurel Technologies WS-650S spin-coater was used to make the spin-cast films. The films were fabricated by preparing 10^{-2} M solutions of each dye and applying ~5 drops of these solutions to circular microscope cover glass slides 25 mm in diameter rotating at 3,000 rpm. The films were dried *in vacuo* for 15 min before further processing and were annealed in the same way as the films on weighing paper. Films for solid-state quantum yield measurements were made in the same way, except they were cast onto circular cover glass slips 13 mm in diameter, as was necessary for our instrument. The sample morphologies of spin-cast films were characterized by Atomic Force Microscopy (AFM) (Digital Image, DI 3000) in tapping mode. The scan area was 20 x 20 μm^2 with a scan rate of 1.00 Hz. The resulting images were processed using Gwyddion software version 2.31.

Samples for X-ray diffraction (XRD) analysis were prepared as follows. The as-isolated (AI) powders were obtained by recrystallization from hexanes/acetone. The AI powders were heated at their predetermined optimum annealing temperatures for 3 h to obtain the thermally annealed (TA) powders. The AI powders were ground in a mortar and pestle for ~30 min to obtain the ground (GR) powders. Spin-cast films subjected to XRD analysis were made from 10^{-2} M dye solutions on 25 mm diameter glass slides as follows: H: ~30 drops, 2,000 rpm; F: ~50 drops, 2,000 rpm; Cl and Br: ~40 drops, 4,000 rpm; I: ~40 drops, 3,000 rpm. XRD patterns for both powders and films were collected using a Panalytical X'Pert Pro MPD diffractometer. The diffractograms were collected as follows: start angle: 10 °, step size: 0.01 °, time/step: 60 s, end angle: 60 °.Differential scanning calorimetry (DSC) was performed on the as-isolated powders using a TA

Instruments DSC 2920 Modulated DSC. The thermograms were recorded using the standard mode. The temperature of the sample chamber was increased at a rate of 5 °C/min from 0 to 200 °C and held isothermic for 10 min. The sample chamber was then cooled at the same rate to 0 °C and held isothermic for 10 min. After the conditioning run, the same protocol was repeated to generate the reported thermograms. Thermograms were analyzed using the Universal Analysis software V 2.3 from TA Instruments.

RESULTS AND DISCUSSION

Optical Properties of Dyes in Solution

The $BF_2dbm(X)OC_{12}H_{25}$ dyes were synthesized via Claisen condensation of 4-dodecyloxyacetophenone with the appropriate halo-ester, followed by boronation in CH_2Cl_2. Purification by recrystallization from hexanes/acetone yielded emissive yellow powders. The absorption and luminescence properties of the compounds were studied in CH_2Cl_2 solution (Table 1). All dyes exhibited high extinction coefficients (>50,000 M^{-1} cm^{-1}) that increased with heavier halogens (Table 1, Fig. S1). There was also a red-shift in absorbance maxima from H to I (Table 1, Fig. S1). The dyes have quantum yields near unity, with the exception of $BF_2dbm(I)OC_{12}H_{25}$,[37] which can be easily explained by the heavy atom effect increasing spin-orbit coupling and thereby decreasing the S_1 population and increasing species population in T_1.[39] All dyes have fluorescence lifetimes between 1.22 and 2.02 ns, fit to single exponential decay (Table 1). There is a slight red shift in fluorescence maxima as the weight of the heavy atom increases (Table 1, Fig. S2).

Table 1 Absorption and Emission Properties of Boron Dyes in CH_2Cl_2 Solution.[a]

Dye	λ_{abs}[b] [nm]	ε [M^{-1} cm^{-1}]	λ_{em}[c] [nm]	φ_F [%]	τ [ns]
H	399[d]	51,600[d]	439[d]	100[d]	2.02[d]
F	400	55,000	435	99	1.77
Cl	404	58,000	441	99	1.22
Br	406	61,000	442	95	1.95
I	409	63,000	444	67[e]	1.50[e]

[a] 369 nm; room temperature, air.
[b] Absorbance maximum.
[c] Emission maximum; fluorescence.
[d] Values taken from reference 33.
[e] Values taken from reference 34.

Mechanochromic Luminescence on Paper

Weighing paper was used as the substrate for dye films to visualize effects with photographs and take measurements at room temperature in air and at 77K in liquid N_2.[37] Previously BF_2bdk dyes were annealed at 110 °C for ML studies.[34,36,37] While the I and H dyes achieved their most blue-shifted emissions and narrowest full widths at half maxima (FWHM) at 110 °C (Fig. 2),[28,36,37] this temperature was found to be insufficient to anneal the F, Cl and Br dyes in this study. For these dyes, different temperatures were tested until a stable maximal blue-shifted emission was found (Fig. 2). Higher temperatures (140 – 150 °C) at or near the melting points for the dyes (Table S1) were required, suggesting that the dyes may be melting and then crystallizing as they cool to form the ordered emissive states. Smeared spectra are essentially the same regardless of annealing temperature. An exemplary smeared emission spectrum is provided for each dye (Fig. 2).

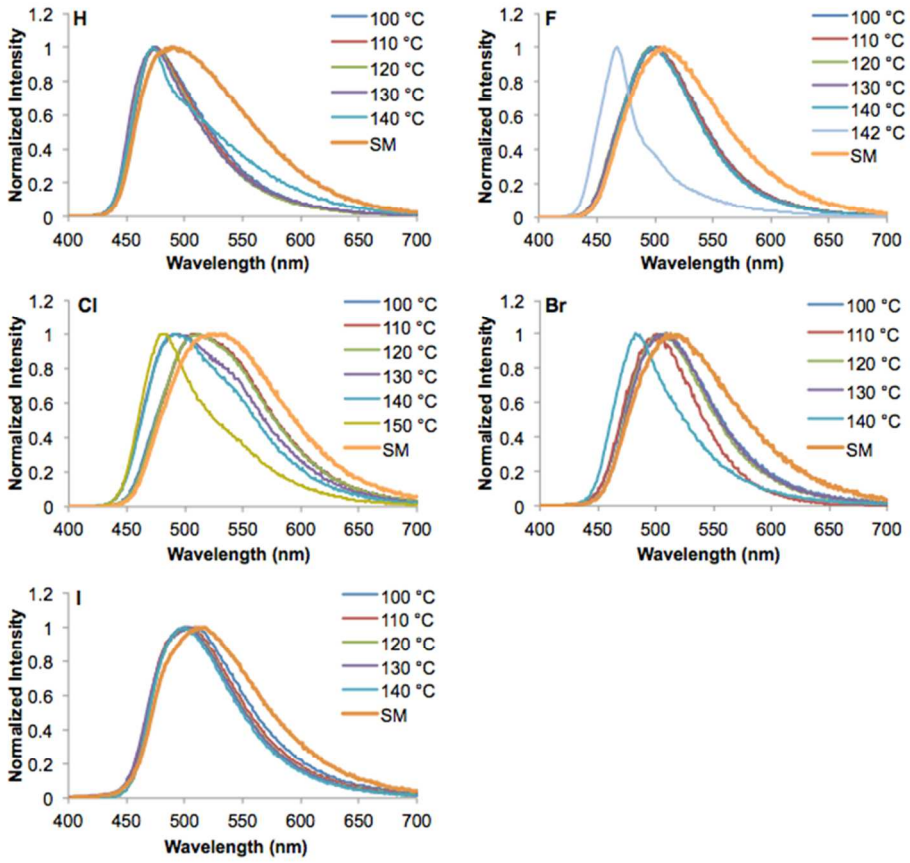

Fig. 2 Emission spectra of $BF_2dbm(X)OC_{12}H_{25}$ dyes as films on weighing paper after annealing for ten minutes at the indicated temperatures (λ_{ex} = 369 nm) (room temperature, air). Note: SM = an exemplary spectrum of the smeared dye film.

As annealed films on weighing paper, the F dye exhibited the most blue-shifted emission (λ_{em} = 467 nm), followed by the H dye (λ_{em} = 475 nm) and more red-shifted heavier halides (Cl and Br: λ_{em} = 483 nm; I: λ_{em} = 502 nm) (Table 2). All dyes exhibited ML at room temperature in air (Fig. S3). When the annealed films were smeared with a cotton swab, their emissions red-shifted (Fig. 3, Table 2). Furthermore, all dyes showed perturbations in their pre-exponential weighted lifetimes (τ_{pw0}) after smearing and emission bands broadened (i.e. increased full widths at half maxima (FWHM)).[41] All lifetimes were fit to multi-exponential decays as is typical for this family of solid-state

dyes (Table S2).[34-36] Such behavior is indicative of either excimer or ground state dimer formation, perhaps H-aggregates as proposed by Zhang *et al.*[6,21,43,44] The H, F, Cl, and Br

Table 2 Luminescence Properties of Dye Films on Weighing Paper.[a]

Dye	Thermally Annealed			Smeared		
	λ_{em}[b] [nm]	τ_{pw0}[c] [ns]	FWHM[d] [nm]	λ_{em} [nm]	τ_{pw0}[c] [ns]	FWHM[d] [nm]
H	475	7.40	65	487	16.0	108
F	467	2.83	36	507	20.0	121
Cl	483	5.13	66	514	13.4	125
Br	483	1.40	63	519	6.66	111
I	502	1.29	87	513	1.01	95

[a] λ_{ex} = 369 nm; room temperature, air.

[b] Emission maximum; fluorescence.

[c] Pre-exponential weighted fluorescence lifetime.[41]

[d] Full Width at Half Maximum.

dyes all showed substantial increases in their pre-exponential weighted lifetimes after smearing while the I dye actually showed a slight decrease in this value. This may be attributed to increased intersystem crossing from S_1 to T_1.[37] As with most BF_2bdk dyes exhibiting ML, the blue-shifted emissions and narrower full widths at half maxima can be recovered by re-annealing with the only visible difference in the materials being mechanical damage and thinning caused by repeated smearing over time (Fig. 3, Fig. S4). The extent of these changes is force and substrate dependent.

The dyes were also tested to see how they responded to multiple cycles of heating and annealing by monitoring their full widths at half maxima. As can be seen in Fig. S4, the F and Cl dyes showed a gradually diminishing ability to respond to mechanical force

after consecutive cycles of annealing and smearing. Repeatedly heating and perturbing the dyes seemed to give them a greater affinity for the ordered emissive state. The H and

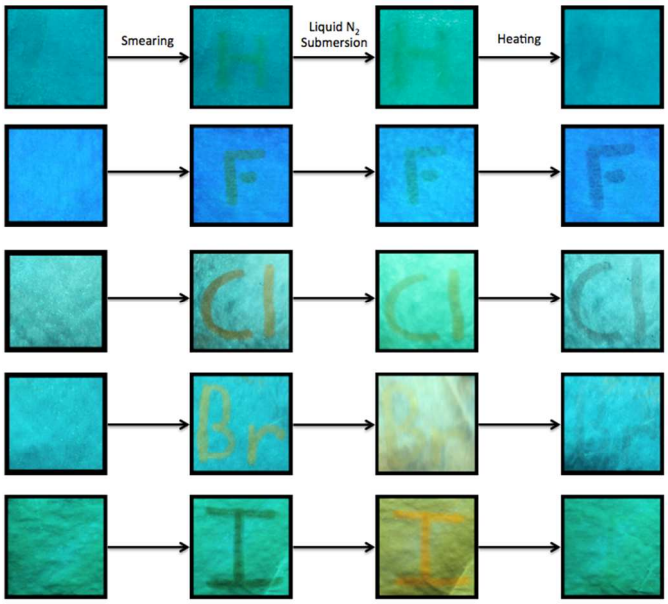

Fig. 3 The $BF_2dbm(X)OC_{12}H_{25}$ dyes as films on weighing paper. Thermally annealed films are smeared, showing mechanochromic luminescence and mechanochromic luminescence quenching (e.g. I). Cooling in liquid nitrogen inhibits oxygen quenching, making phosphorescence visible (e.g. I). Heating facilitates erasure.

Br dyes, on the other hand, continued to respond to mechanical force through seven cycles. The I dye did not show a particularly large bathochromic shift or increase in FWHM after smearing on weighing paper and showed only a slight decrease in its ability to respond to smearing over time. As previously described for $BF_2dbm(I)OC_{12}H_{25}$, all of the dyes showed a decrease in fluorescence intensity after smearing at room temperature under air (the emission and excitation slit widths were kept the same for the TA and SM spectra of each dye, respectively) suggesting that mechanical force leads to fluorescence quenching to some extent, likely through mechanically induced changes in dye aggregation that enhance intersystem crossing to the triplet excited state.[37] At first glance, this drop in intensity could be attributed to simply removing emissive material with

smearing. However, because the intensities increased again after re-annealing (Fig. S5), there must be more to this phenomenon.

The luminescence properties of the dyes were also examined at 77K in liquid N_2. This was necessary to study the effect of mechanical perturbation on triplet emission because, at room temperature under air, the phosphorescence of these dyes is diminished by a combination of collisional O_2 quenching and non-radiative decay from the triplet state.[37] As can be seen in Fig. 3, the smeared portion of the I dye undergoes a marked change from dim to bright orange when submerged in liquid N_2. When examining the total emission spectra of the I and Br dyes at 77K in liquid N_2, blue-shifted peaks corresponding to fluorescence and red-shifted peaks corresponding to phosphorescence are observed (Fig. 4; λ_{em} fluorescence: I dye, annealed: ~490 nm, smeared: ~500 nm; Br dye, annealed: ~500 nm, smeared: ~530 nm. λ_{em} phosphorescence = ~560-580 nm when annealed or smeared for both dyes). To clarify, the H, F, and Cl dyes also exhibit phosphorescence under these conditions, evidenced by delayed emission spectra (Fig. S6), but the fluorescence signal is too strong relative to phosphorescence for it to be observed in a total emission scan. As can be seen in Fig. 4, smearing the annealed films of the Br and I dyes produces the aforementioned red-shift in fluorescence as well as a change in F/P that can be observed in liquid N_2. Furthermore, the smeared Br dye film shows an unusually large FWHM after smearing (FWHM = 123 nm) compared to the others in the total emission scan (Table S3). This may be indicative of a greater degree of excimer or other aggregate formation in this dye upon mechanical perturbation.

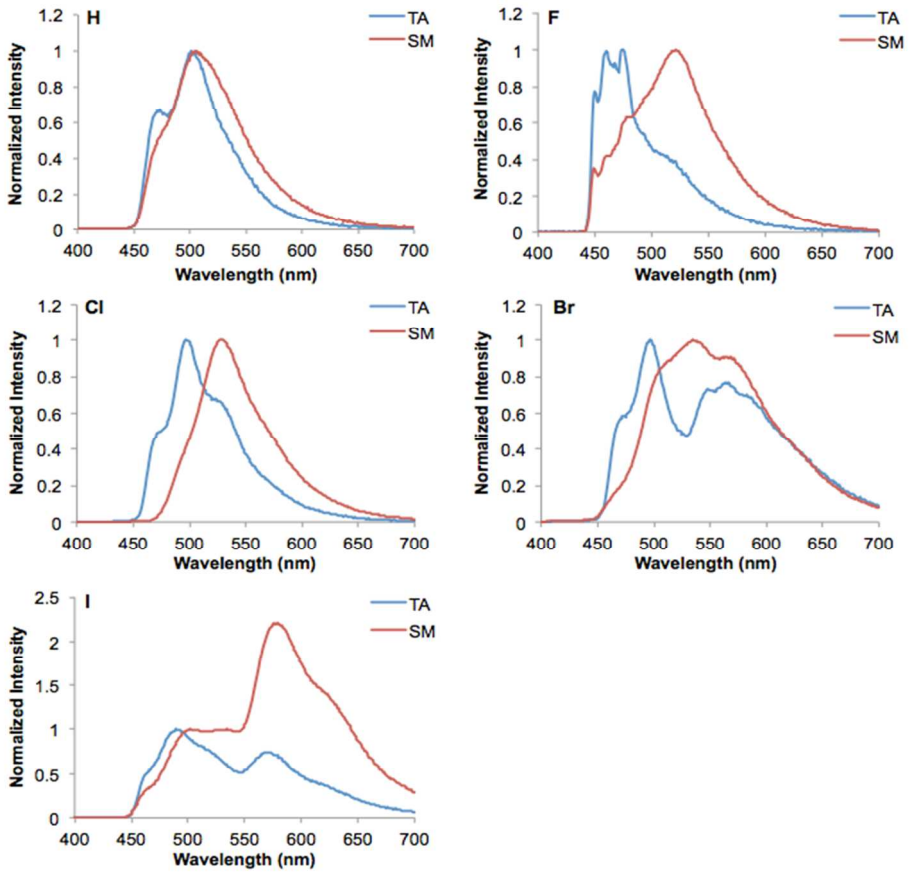

Fig. 4 Normalized total emission spectra of boron dyes on weighing paper in both thermally annealed (TA) and smeared (SM) states (λ_{ex} = 369 nm) (77K, liquid N_2). Spectra are normalized to their corresponding fluorescence maxima (i.e. singlet emission).

Interestingly, the intensities of the phosphorescence peaks increase for every dye studied when the thermally annealed sample is smeared (Fig. 5). The emission and excitation slit widths were kept the same for the TA and SM spectra for each dye, making this comparison possible. The change in F/P intensity ratio could only be observed in a total emission scan at 77K in liquid N_2 for the Br and I dyes. The expected trend was noted in the phosphorescence lifetimes of the annealed films. As the weight of the heavy atom substituent increased, the phosphorescence lifetimes decreased (i.e. H = 463 ms, F = 244 ms, Cl = 208 ms, Br = 42.6 ms, and I = 14.4 ms) (Table S4). This trend is commonly

observed for halide substituted luminescent, aromatic organic compounds.[45,46] In Table S4 and Fig. S6, it can be seen that the delayed emission maxima of all dyes change very little in response to mechanical force, while their pre-exponential weighted phosphorescence lifetimes increase dramatically. This shows that the energy of the aggregate T_1 excited state is not changing in a significant way but the population of excited-state species in T_1 is increasing in response to mechanical force. We have previously put forth that a lowering of the energy of the aggregate S_1 excited state in response to mechanical force could increase intersystem crossing between S_1 and T_1 in the presence of a heavy atom, and that this is a possible explanation for the mechanism of MLQ.[37,47] These data strongly support that claim. Furthermore, we show that MLQ is a phenomenon not limited to the iodine substituted BF_2dbm(I)$OC_{12}H_{25,}$ but extends to dyes with lighter halogen substituents and, to our initial surprise, even to a dye without any heavy atom at all. The iodine substituent simply makes this effect visible to the unaided eye at both room temperature in air and at 77K in liquid N_2.

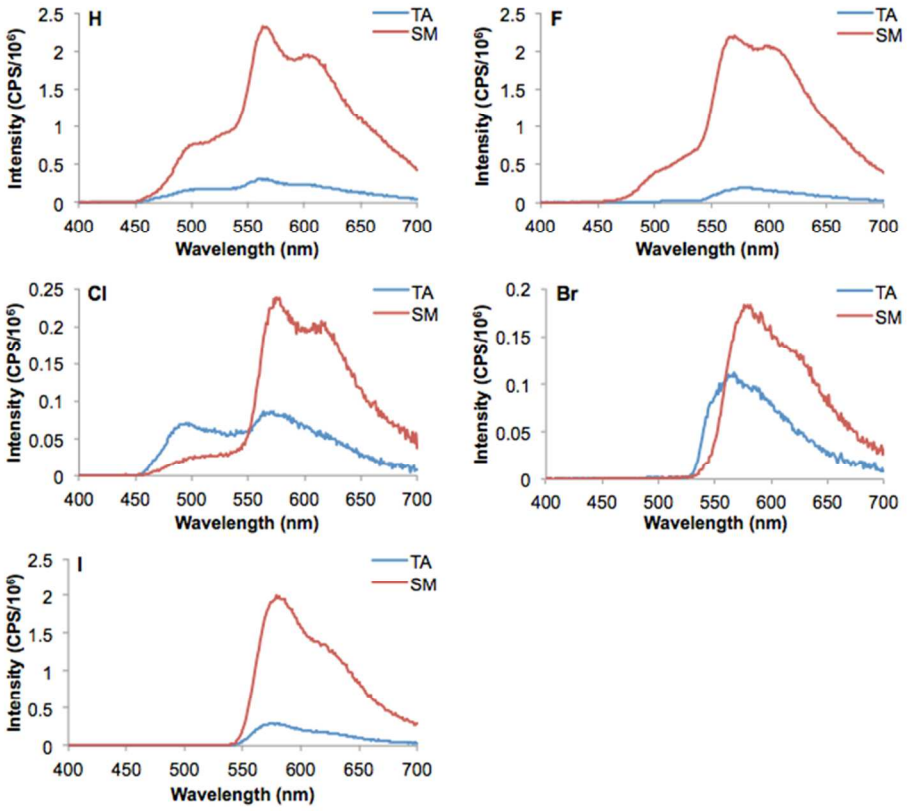

Fig. 5 Delayed emission spectra of boron dyes on weighing paper in both thermally annealed (TA) and smeared (SM) states (λ_{ex} = 369 nm) (77K, liquid N_2). The intensities were recorded in photon counts per second (CPS) and shown as CPS/10^6.

Mechanochromic Luminescence on Glass

In order to study substrate effects, measure solid-state quantum yields, investigate the spontaneous recovery of the dye materials after smearing, and to acquire images of the materials in various states using atomic force microscopy (AFM), thin spin-cast films on microscope cover glass were utilized. Fluorescence spectra of the films were recorded and a blue-shift, narrowing of the full widths at half maxima, and shortening of the pre-exponential weighted lifetimes (with the exception of the I dye for which the lifetime actually increased) were observed upon annealing the as-spun films (Fig. 6, Table S5).

Also, all dyes had more blue-shifted fluorescence maxima in the TA state as spin-cast films than they did as films on weighing paper, which is an interesting processing effect.

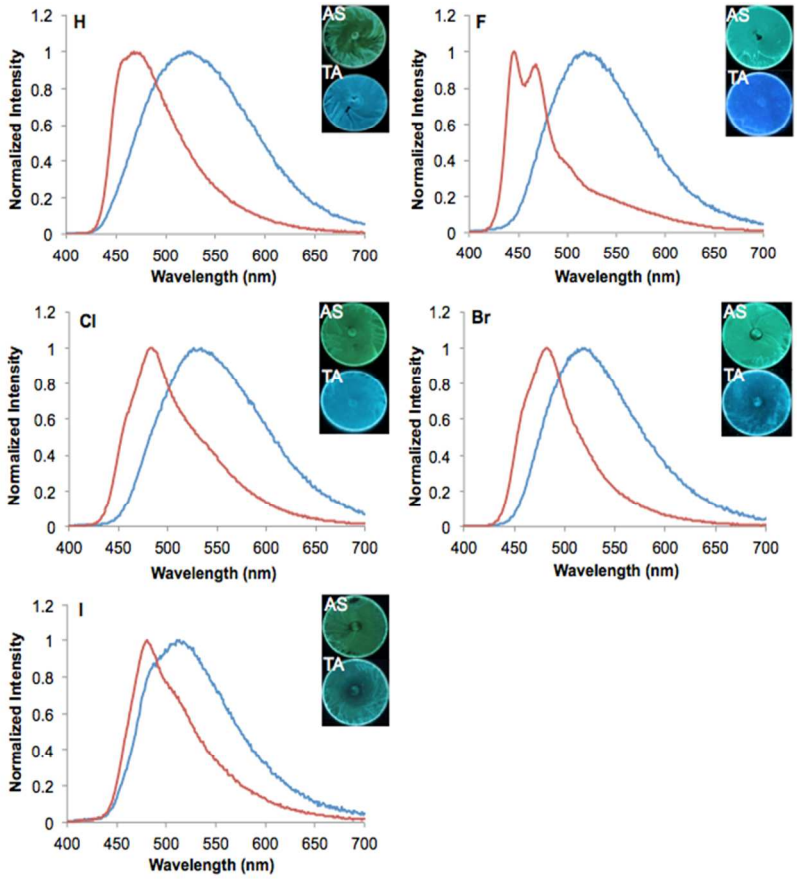

Fig. 6 Normalized emission spectra of boron dyes as spin-cast films on microscope cover glass in both as-spun (AS) and thermally annealed (TA) states (λ_{ex} = 369 nm) (room temperature, air).

Perhaps the dye molecules show a greater propensity to adhere to each other and form crystallites when on glass substrates, compared to paper where there may be stronger interactions with the fibrous cellulose substrate. The annealed F dye on glass exhibits the same peak at ~467 nm as on weighing paper. However, a more blue-shifted peak at 445 nm is also present in the spectrum. This may be a thickness effect due to increased self-absorption causing the loss of the blue-shifted peak in the thicker film on weighing paper.[34]

Solid-state quantum yields were collected for the spin-cast films. The quantum yields were measured after annealing and then again after smearing the films (Table 3). Both annealed and smeared films exhibited trends typically associated with the heavy atom effect. Films of the H dye had the highest quantum yields (~50-68%), films of the F and Cl dyes had intermediate quantum yields (~34-46%), and films of the Br and I dyes had the lowest quantum yields (~2-13%). As was expected, the H, F, Cl, and I dyes all experienced a decrease in quantum yield corresponding to smearing, consistent with MLQ. Interestingly, the Br dye showed anomalous behavior compared to the others, exhibiting a slight increase (~3%) in quantum yield upon smearing. This data, combined with the fact that the dye also appears to become slightly brighter to the naked eye upon smearing (Fig. 3), suggests that the ML properties of this dye are more complex. Other data suggest that smearing enhances cross-over to the triplet state in this dye as evidenced by the increase in intensity and lifetime of the delayed emission spectrum at 77K in liquid N_2 as well as the decrease in F/P that was observed in a total emission spectrum recorded under the same conditions (Fig. 4, Fig. 5, Table S4). Thus, it seems likely that some quenching of phosphorescence is occurring when the annealed sample is smeared at room temperature under air. However, the increased quantum yield for the bromine dye may point to excimer or other aggregate formation unique among the dye set upon smearing. Perhaps certain aggregates are more efficient singlet emitters making intersystem crossing to their triplet states less efficient.

Just as has been previously observed with BF_2bdk dyes exhibiting ML, the transition from as-spun to thermally annealed films seems to correspond to a change from relatively amorphous to a more ordered material.[36] This was confirmed by analyzing

spin-cast films of the dyes using atomic force microscopy (AFM) (Fig. 7). As can be seen from the AFM images, all dyes show a significant growth of crystallites after annealing. The F and Cl dyes form rather large, lamellar crystallites by comparison to the other dyes, which form smaller, needle-like crystallites. A possible explanation for this could be that the smaller, more electronegative halogen substituents provide greater stability for more highly organized dye aggregates via halogen-hydrogen and halogen-halogen interactions. In fact, $BF_2dbm(H)OC_{12}H_{25}$ molecules are already known to exhibit C−H•••F bonding between the ortho carbon of the phenyl ring on one molecule and the BF_2 moiety on another in the solid state resulting in the observation of lamellar structures when studied using scanning tunneling microscopy (STM).[48] Furthermore, Saccone *et al.* have reported crystal structures of azobenzene compounds that exhibit intermolecular F•••F bonding and bifurcated H•••F•••H bonds.[49] It should also be noted that the Br dye film exhibits a relatively high degree of organization in the AS state compared to the others, as evidenced by blocky crystallites in the AFM image.

Table 3 Solid State Luminescence Quantum Yields for the Dyes as Spin-Cast Films on Glass at Room Temperature Under Air.[a]

Dye	Thermally Annealed φ[b] [%]	Smeared φ [%]
H	67.66	49.53
F	38.33	35.80
Cl	46.06	33.93
Br	9.71	13.23
I	8.10	2.37

[a] λ_{ex} = 369 nm.
[b] Solid state luminescence quantum yield.

Boron dyes of this type are known to possess the ability to spontaneously return to more blue-shifted emissive states after smearing at room temperature.[35,36] Furthermore,

BF_2dbm(H)$OC_{12}H_{25}$ and BF_2AVB have been shown to recover spontaneously at room temperature as thin films on paper and on glass.[34,35] For this study, the spontaneous recovery of the dyes was studied as spin-cast films on glass. The dyes were annealed at their predetermined optimum temperatures and then their recovery was monitored for a period of three weeks after which they were annealed a second time. It was found that all of the dyes were able to spontaneously recover blue-shifted emissive states to some extent (Fig. S7). Out of all of the dyes studied, the H dye showed the greatest ability to recover spontaneously, reaching an emission maximum within 10 nm of that of the TA state after 16 days. The dyes with halogen substituents showed a much more limited ability to recover, with the Cl, Br, and I dyes ceasing to recover after one week and only getting to within ~25 nm of the TA emissions. The F dye also ceased to recover further after one week and only got to within 53 nm of the TA emission wavelength. When re-annealed after three weeks, all of the dyes recovered their ordered emissive states with the exception of the I dye. This dye seemed to lose its ability to recover. This could be due to its decreased affinity for forming the more organized lamellar crystallites compared to the other dyes, as evidenced by the AFM images (Fig. 7). Once again, this suggests that these dyes have a greater affinity for the ordered emissive state after re-annealing. The fact that these dyes either don't fully recover at room temperature or do so very slowly could potentially make them useful for applications where a longer lasting inscription is desirable. For example, a billboard in a restaurant or café could be inscribed with the specials of the day and then heated at the end of the day to erase. X-ray Diffraction (XRD) techniques were also used to study the dyes as spin-cast films on glass. In order to obtain sufficient signal strength using this technique, it was necessary to

make thicker films of the dyes than those used for studying the optical properties. The optimal method for producing such films was determined empirically and varied on a case-by-case basis. These differences may be attributed to observed variations in solubility and aggregation tendencies among the dyes. As expected, the films were most crystalline after annealing and most amorphous after smearing. The F dye showed the most drastic change going from as-spun to thermally annealed and then to smeared (Fig. 8). When this dye was annealed, a strong peak arose at ~12.6 ° and a much weaker yet clearly distinguishable peak appeared at ~18.8 °. When the thermally annealed sample was smeared, these peaks disappeared. The I dye also showed clear signs of crystallinity in both the AS and TA films (Fig. 8). In the as-spun film, there are three intense peaks at ~13.9 °, ~10.4 ° and ~27.8 °. When this sample is annealed, these peaks become more intense and their relative ratios change. Again, when the sample is smeared it becomes amorphous and no peaks are evident. XRD data for H, Cl, and Br are provided in Fig. S8.

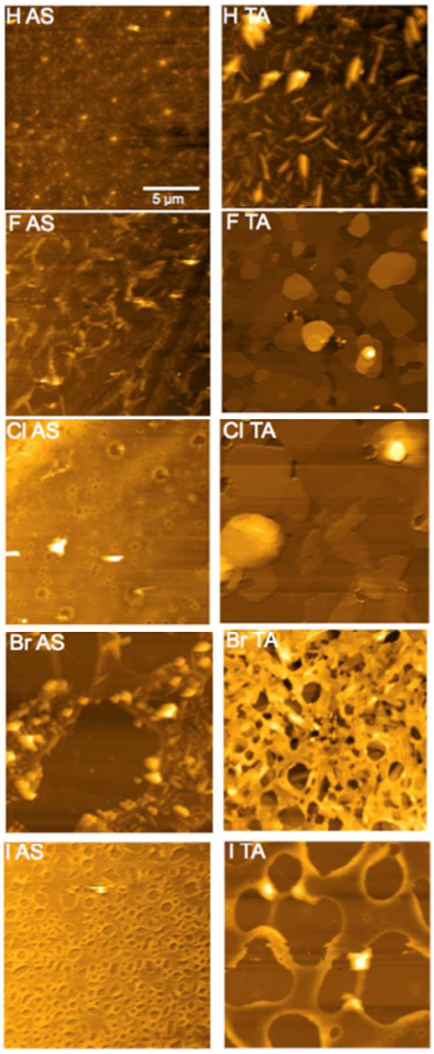

Fig. 7 AFM images of boron dyes as spin-cast films on glass in both as-spun (AS) and thermally annealed (TA) states.

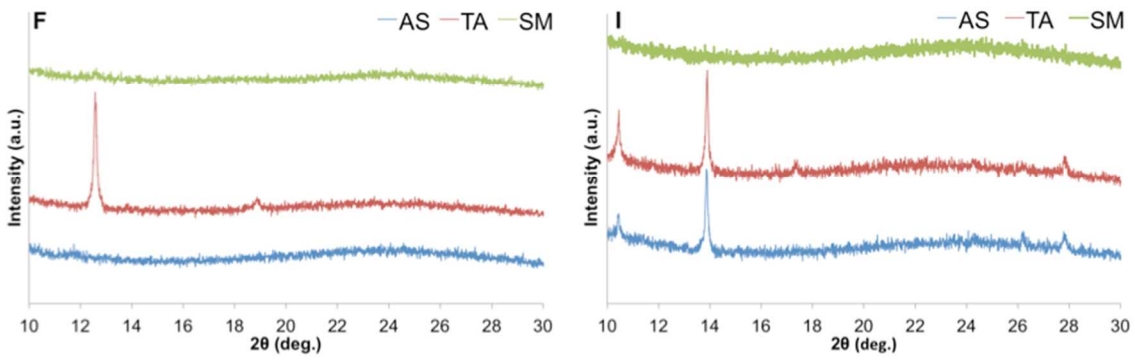

Fig. 8 X-ray diffraction (XRD) patterns of the F and I dyes as-spun (AS), thermally annealed (TA), and smeared (SM).

Mechanochromic Luminescence of Bulk Powders

Just like the films on weighing paper and glass substrates, the emissions of the bulk powders also responded to annealing and mechanical stress to varying degrees (Table S6, Fig. S9, and Fig. S10). However, more rigorous thermal and mechanical conditions were required to induce emission changes in powders. Compared to films, bulk powders required longer annealing times (i.e. 3 hours) in order to achieve stable, maximal blue-shifts in emission. Typical trends are observed upon annealing (blue-shift) and smearing (red-shift) (Fig. 9). Powders also required vigorous grinding with a mortar and pestle for ~30 minutes to achieve typical red-shifts in emission. The same emissions were observed whether as-isolated or thermally annealed powders were ground.

Powder samples were also subjected to XRD analysis to assess structural factors such as crystallinity. To prepare as-isolated and thermally annealed samples for XRD analysis it was necessary to lightly chop the powders with a razor blade for ~1 minute. Importantly, this did not produce the red-shifts in emission observed for the ground samples. The most notable differences for the bulk powders can be observed by comparing the XRD patterns for thermally annealed and as-isolated forms with the

ground sample patterns (Fig. 10). In general, the as-spun and thermally annealed diffractograms have many more distinct, strong peaks suggesting crystallinity. The diffractograms of the ground samples, on the other hand, show fewer peaks and a general decrease in diffraction intensity. This suggests that the ground samples are more amorphous, as expected.

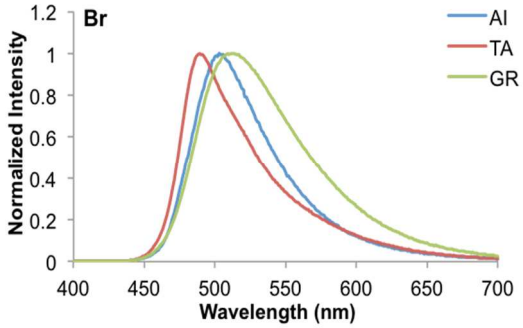

Fig. 9 Emission spectra of the Br dye as a bulk powder (λ_{ex} = 369 nm) (room temperature, air). As-isolated (AI), thermally annealed (TA), and ground (GR) powders are compared.

From analyzing the XRD diffractograms of the dyes in all three forms, it was concluded that the as-isolated samples represent a mixture of both amorphous and ordered emissive species. In almost every case, peaks unique to thermally annealed or ground samples are both present in the diffractograms of the as-isolated samples. Using the diffractograms of the Br dye as an example, a distinctly structured peak is present at ~14.5 ° in both the AI and GR samples, but this peak is absent from the diffractogram of the TA sample (Fig. 10). In addition to this, there is a distinctly structured peak at ~18.4 ° in the AI diffractogram that becomes more intense in the TA diffractogram, but is absent from the GR diffractogram. Credence is also lent to this idea by studying the emission spectra of the Br bulk powder sample in all three forms; the AI emission spectrum is

intermediate in relation to the other two and overlaps considerably with both of them (Fig. 9).

The H dye bulk powder is anomalous in that it shows very little change in its emission spectrum in response to both heating and mechanical force. This is reflected in the XRD patterns where the AI, TA, and GR diffractograms are practically identical, barring changes in overall intensity. The only significant difference between the patterns is seen in the GR sample where the peak at ~19.1 ° increases in relative intensity. The I dye is unique as well because it shows very little change in its emission or XRD diffractograms when the AI powder is annealed. Once again, this correlates with the AFM data to suggest that the I dye has less affinity for forming a crystalline, ordered emissive state upon annealing. However, the GR emission spectrum is red-shifted and the XRD pattern suggests a significant decrease in crystallinity.

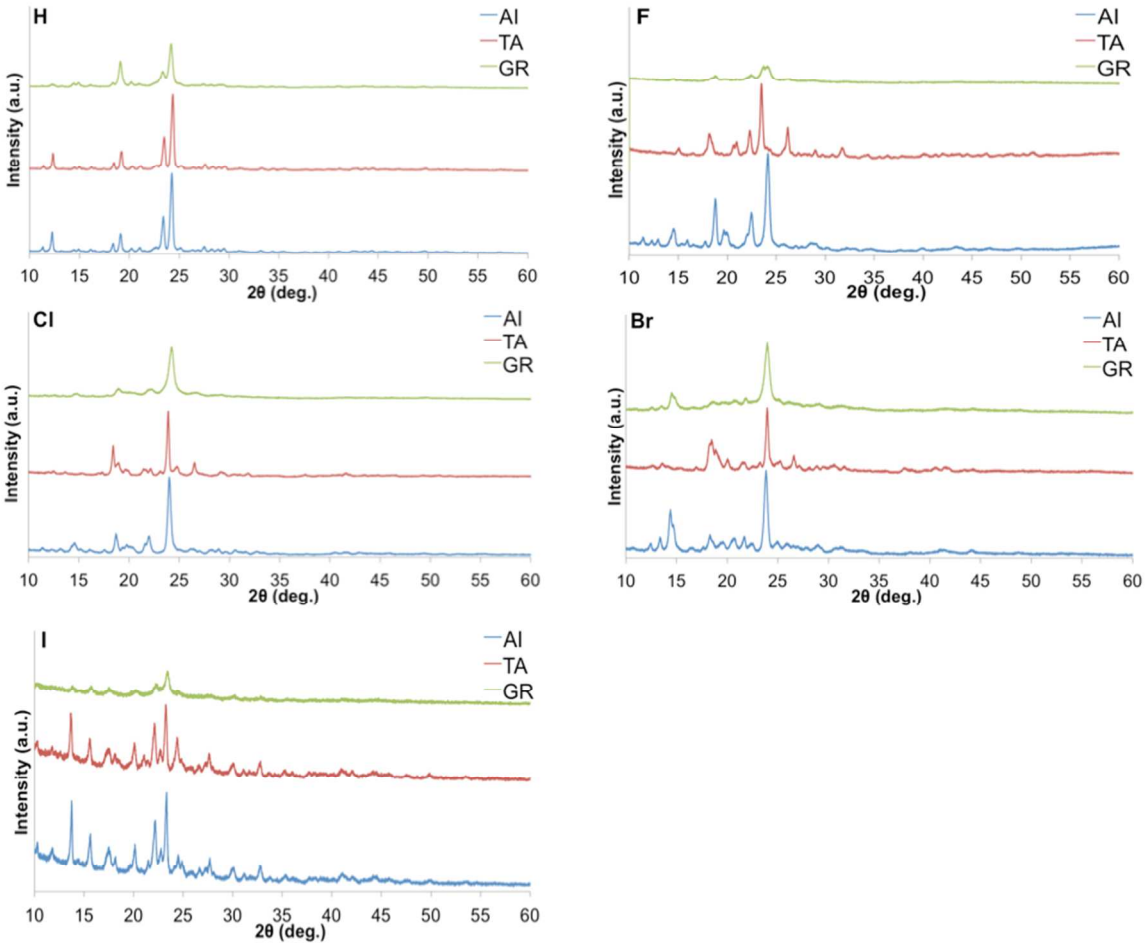

Fig. 10 Powder X-ray diffraction (XRD) patterns of the boron dyes as bulk powders in their as-isolated (AI), thermally annealed (TA), and ground (GR) states.

Differential Scanning Calorimetry of Powders

In order to gain a greater understanding of the thermal properties of the dyes, differential scanning calorimetry (DSC) measurements were carried out on the bulk, AI powders. TA and GR powders were also studied, but showed no significant differences. The results are summarized in Table 4 and the thermograms are displayed in the supporting information (Fig. S11). All dyes showed melting points (T_m) in the range of ~135-156 °C and crystallization temperatures (T_c) between ~110-144 °C. Interestingly, strong transitions can be

observed in the 2nd cycles of the F and I samples in addition to their melting and crystallization. The exact nature of these transitions is difficult to decipher, but they are most likely not transitions to liquid crystalline states because their respective enthalpies are much too large.[50]

Table 4 Differential Scanning Calorimetry Data for As-Isolated Dyes.[a]

Dye	T_m[b] (ΔH[c])	T_c[d] (ΔH[c])
H	134.66 (560.0)	109.81 (573.7)
F	145.47 (314.9)	140.45 (308.4)
Cl	156.05 (432.3)	143.82 (414.3)
Br	153.76 (375.3)	136.89 (386.5)
I	151.87 (289.9)	141.91 (266.8)

[a] All data was taken from the 2nd cycle.
[b] Melting point given in °C as the peak of the major endothermic transition.
[c] Enthalpy of the transition given in kJ/mol.
[d] Crystallization point given in °C as the peak of the major exothermic transition.

Summary

In conclusion, a series of lipid derivative BF_2bdk dyes with and without halide substituents were synthesized and all were found to exhibit MLQ, demonstrating that the effect is not limited to BF_2dbm(I)$OC_{12}H_{25}$.[37] In fact, it may be universal to all BF_2bdk dyes exhibiting ML due to mechanical force creating aggregates with lower energy S_1 excited states while the energy of the aggregate T_1 excited states remain, by and large, unchanged.[21] Furthermore, it was found that films on weighing paper of the dyes with F, Cl, and Br substituents required higher temperatures to anneal than those with H or I substituents. Annealed spin-cast films on microscope cover glass of the F and Cl dyes also exhibited relatively large and organized lamellar crystallites by comparison to their H, Br, and I counterparts when examined by AFM. Spin-cast films of the dyes with halogen substituents

showed a slower recovery of their ordered emissive states after smearing under ambient conditions compared to the hydrogen analogue. This ability to tune fading time could make them useful for applications in which a more permanent inscription is desirable. Spin-cast films of the H, F, Cl, and I dyes also showed a decrease in quantum yield upon smearing the annealed sample. The Br dye, on the other hand, exhibited a slight increase in quantum yield upon smearing suggesting the formation of unique aggregate species. Finally, XRD data collected for both bulk powders and spin-cast films on glass revealed a transition from a relatively amorphous state to a state with a higher degree of crystallinity after thermally annealing the AI powders and films. The crystallinity of the samples was further reduced after the AI powders were ground using a mortar and pestle. In many cases, the AI powder samples contained both ordered and amorphous features in XRD patterns and emission spectra. The mechanoresponsive properties of BF_2bdk dyes remain a topic of on-going study to gain a greater understanding of these materials and their possible applications.

Acknowledgements

We thank the National Science Foundation (CHE GA11015) for support for this research. Dr. Jiwei Lu is acknowledged for his guidance with AFM measurements. Dr. Michal Sabat is acknowledged for his guidance with XRD measurements. We also thank Ziyi Fan, Christopher DeRosa, Tristan Butler, and Milena Kolpaczynska for their assistance and helpful discussions.

Notes and references

[a] Department of Chemistry, University of Virginia, McCormick Road, Charlottesville, Virginia 22904, United States.

† Synthesis and characterization data for the dyes are provided in the ESI.

(1) Chi, Z.; Zhang, X.; Xu, B.; Zhou, X.; Ma, C.; Zhang, Y.; Liu, S.; Xu, J. *Chem. Soc. Rev.* **2012**, *41*, 3878.
(2) Yoshimitsu, S.; Takashi, K. *Nat. Chem.* **2009**, *1*, 605.
(3) Kinami, M.; Crenshaw, B. R.; Weder, C. *Chem. Mater.* **2006**, *18*, 946.
(4) Black, A. L.; Lenhardt, J. M.; Craig, S. L. *J. Mater. Chem.* **2011**, *21*, 1655.
(5) Davis, D. A.; Hamilton, A.; Yang, J.; Cremar, L. D.; Van Gough, D.; Potisek, S. L.; Ong, M. T.; Braun, P. V.; Martínez, T. J.; White, S. R.; Moore, J. S.; Sottos, N. R. *Nature* **2009**, *459*, 68.
(6) Sagara, Y.; Kato, T. *Angew. Chem. Int. Ed.* **2008**, *47*, 5175.
(7) Sagara, Y.; Yamane, S.; Mutai, T.; Araki, K.; Kato, T. *Adv. Funct. Mater.* **2009**, *19*, 1869.
(8) Löwe, C.; Weder, C. *Adv. Mater.* **2002**, *14*, 1625.
(9) Crenshaw, B. R.; Weder, C. *Chem. Mater.* **2003**, *15*, 4717.
(10) Ito, H.; Saito, T.; Oshima, N.; Kitamura, N.; Ishizaka, S.; Hinatsu, Y.; Wakeshima, M.; Kato, M.; Tsuge, K.; Sawamura, M. *J. Am. Chem. Soc.* **2008**, *130*, 10044.
(11) Ni, J.; Zhang, X.; Qiu, N.; Wu, Y.-H.; Zhang, L.-Y.; Zhang, J.; Chen, Z.-N. *Inorg. Chem.* **2011**, *50*, 9090.
(12) Sagara, Y.; Komatsu, T.; Ueno, T.; Hanaoka, K.; Kato, T.; Nagano, T. *J. Am. Chem. Soc.* **2014**, *136*, 4273.
(13) Hong, Y.; Lam, J. W. Y.; Tang, B. Z. *Chem. Soc. Rev.* **2011**, *40*, 5361.
(14) Hong, Y.; Lam, J. W. Y.; Tang, B. Z. *Chem. Commun.* **2009**, 4332.
(15) Luo, J.; Xie, Z.; Lam, J. W. Y.; Cheng, L.; Chen, H.; Qiu, C.; Kwok, H. S.; Zhan, X.; Liu, Y.; Zhu, D.; Tang, B. Z. *Chem. Commun.* **2001**, 1740.
(16) Li, D.; Liang, Z.; Chen, J.; Yu, J.; Xu, R. *Dalton Trans.* **2013**, *42*, 9877.
(17) Huang, J.; Sun, N.; Chen, P.; Tang, R.; Li, Q.; Ma, D.; Li, Z. *Chem. Commun.* **2014**, *50*, 2136.
(18) Zhao, Z.; Chen, S.; Lam, J. W. Y.; Lu, P.; Zhong, Y.; Wong, K. S.; Kwok, H. S.; Tang, B. Z. *Chem. Commun.* **2010**, *46*, 2221.
(19) Chung, J. W.; You, Y.; Huh, H. S.; An, B.-K.; Yoon, S.-J.; Kim, S. H.; Lee, S. W.; Park, S. Y. *J. Am. Chem. Soc.* **2009**, *131*, 8163.
(20) Yoon, S.-J.; Park, S. *J. Mater. Chem.* **2011**, *21*, 8338.
(21) Sun, X.; Zhang, X.; Li, X.; Liu, S.; Zhang, G. *J. Mater. Chem.* **2012**, *22*, 17332.
(22) Xue, P.; Yao, B.; Sun, J.; Xu, Q.; Chen, P.; Zhang, Z.; Lu, R. *J. Mater. Chem. C* **2014**, *2*, 3942.
(23) Qi, Q.; Zhang, J.; Xu, B.; Li, B.; Zhang, S. X.-A.; Tian, W. *J. Phys. Chem. C* **2013**, *117*, 24997.
(24) Halik, M.; Wenseleers, W.; Grasso, C.; Stellacci, F.; Zojer, E.; Barlow, S.; Bredas, J.-L.; Perry, J. W.; Marder, S. R. *Chem. Commun.* **2003**, 1490.

(25) Cogné-Laage, E.; Allemand, J.-F.; Ruel, O.; Baudin, J.-B.; Croquette, V.; Blanchard-Desce, M.; Jullien, L. *Chem. Eur. J.* **2004**, *10*, 1445.
(26) Chow, Y. L.; Johansson, C. I.; Zhang, Y.-H.; Gautron, R.; Yang, L.; Rassat, A.; Yang, S.-Z. *J. Phys. Org. Chem.* **1996**, *9*, 7.
(27) Ono, K.; Yoshikawa, K.; Tsuji, Y.; Yamaguchi, H.; Uozumi, R.; Tomura, M.; Taga, K.; Saito, K. *Tetrahedron* **2007**, *63*, 9354.
(28) Liu, T.; Chien, A. D.; Lu, J.; Zhang, G.; Fraser, C. L. *J. Mater. Chem.* **2011**, *21*, 8401.
(29) Xu, S.; Evans, R. E.; Liu, T.; Zhang, G.; Demas, J. N.; Trindle, C. O.; Fraser, C. L. *Inorg. Chem.* **2013**, *52*, 3597.
(30) Zhang, G.; Chen, J.; Payne, S. J.; Kooi, S. E.; Demas, J. N.; Fraser, C. L. *J. Am. Chem. Soc.* **2007**, *129*, 8942.
(31) Samonina-Kosicka, J.; DeRosa, C. A.; Morris, W. A.; Fan, Z.; Fraser, C. L. *Macromolecules* **2014**, *47*, 3736.
(32) Zhang, X.; Liu, X.; Lu, R.; Zhang, H.; Gong, P. *J. Mater. Chem.* **2012**, *22*, 1167.
(33) Liu, X.; Zhang, X.; Lu, R.; Xue, P.; Xu, D.; Zhou, H. *J. Mater. Chem.* **2011**, *21*, 8756.
(34) Zhang, G.; Singer, J. P.; Kooi, S. E.; Evans, R. E.; Thomas, E. L.; Fraser, C. L. *J. Mater. Chem.* **2011**, *21*, 8295.
(35) Zhang, G.; Lu, J.; Sabat, M.; Fraser, C. L. *J. Am. Chem. Soc.* **2010**, *132*, 2160.
(36) Nguyen, N. D.; Zhang, G.; Lu, J.; Sherman, A. E.; Fraser, C. L. *J. Mater. Chem.* **2011**, *21*, 8409.
(37) Zhang, G.; Lu, J.; Fraser, C. L. *Inorg. Chem.* **2010**, *49*, 10747.
(38) Liang, W. Y. *Phys. Educ.* **1970**, *5*, 226.
(39) Lower, S. K. E.-S., M.A. *Chem. Rev.* **1966**, 199.
(40) Williams, D. B. G.; Lawton, M. *J. Org. Chem.* **2010**, *75*, 8351.
(41) Carraway, E. R.; Demas, J. N.; DeGraff, B. A.; Bacon, J. R. *Anal. Chem.* **1991**, *63*, 337.
(42) Zhu, H.; Wang, X.; Li, Y.; Wang, Z.; Yang, F.; Yang, X. *Chem. Commun.* **2009**, *0*, 5118.
(43) Mirochnik, A. G.; Bukvetskii, B. V.; Fedorenko, E. V.; Karasev, V. E. *Russ. Chem. Bull.* **2004**, *53*, 291.
(44) Lakowicz, J. R. *Principles of Fluorescence Spectroscopy*; Springer: New York, Ny, 2007.
(45) McClure, D. S. *J. Chem. Phys.* **1949**, *17*, 905.
(46) Ventura, B.; Bertocco, A.; Braga, D.; Catalano, L.; d'Agostino, S.; Grepioni, F.; Taddei, P. *J. Phys. Chem. C* **2014**, *118*, 18646.
(47) Zhang, G.; Palmer, G. M.; Dewhirst, M. W.; Fraser, C. L. *Nat. Mater.* **2009**, *8*, 747.
(48) Zhang, X.; Yan, C.-J.; Pan, G.-B.; Zhang, R.-Q.; Wan, L.-J. *J. Phys. Chem. C* **2007**, *111*, 13851.
(49) Saccone, M.; Terraneo, G.; Pilati, T.; Cavallo, G.; Priimagi, A.; Metrangolo, P.; Resnati, G. *Acta Crystallogr., Sect. B: Struct. Sci.* **2014**, *70*, 149.
(50) Singh, S. *Phys. Rep.* **2000**, *324*, 107.

Graphical Abstract

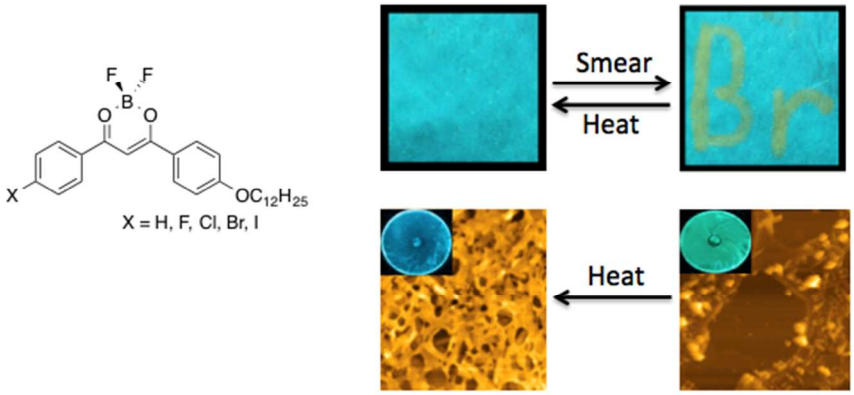

Halide-substituted difluoroboron β-diketonates were synthesized and display mechanochromic luminescence and quenching. Material structure is halide dependent and dynamic recovery properties for halide dyes are slower than for the hydrogen counterpart.